JOURNAL OF COMPUTATIONAL PHYSICS 33, 397–404 (1979)

Note

A Graphical Method for Finding Complex Roots and Its Application to Plasma Physics Problems

A graphical method is described for finding the complex roots of a nonlinear equation: $g(\omega) = 0$. Basically a mesh of potential roots, ω, is chosen; values of g on this mesh are calculated; and the zero contours of $\mathrm{Re}(g)$ and $\mathrm{Im}(g)$ are plotted. The intersections of these contours are the desired roots, or possibly singularities. The primary advantage of the method is that it provides the complete spectrum of roots or eigenvalues within a specified range of ω-space. The method is easy to apply, provided a reliable contour plotting routine is available, and is quite efficient whenever g is inexpensive to evaluate. Application of the method is illustrated by two example problems from plasma physics.

1. Introduction

A frequently occurring problem is that of finding the roots to a nonlinear equation, i.e., solving for the ω values that satisfy $g(\omega) = 0$, where g is nonlinear. Starting from a reasonable guess, Newton's method [1] is an efficient way of finding a single root. Additional roots, when present, can be obtained by changing the initial guess appropriately. Alternatively, if one is interested in only a particular range of ω values, one can plot $g(\omega)$ over that range and obtain all the roots graphically.

Sometimes g and ω are complex. In such cases the problem is equivalent to finding the vector roots of a system of two nonlinear equations. Again generalization of Newton's method [1] can be used. However, such methods will still give only a single root at a time, and their convergence is typically even more sensitive to the accuracy of the initial guess than in the real or scalar case. Consequently, the root (s) of most interest might not be found.

For the case of complex roots, a simple graphical method is also available. This method, which is described here, has the advantage of giving all the roots within a specified region of the ω-plane. One is thus assured that important roots are not overlooked. The method is easily implemented on a computer, provided a reliable contour plotting routine is available, and is practical as long as the evaluation of $g(\omega)$ is not too time consuming.

2. Description of Method

To apply the graphical method, one first chooses a region of the ω-plane in which the roots are desired. Next, a mesh of ω values is overlaid on the region, and $g(\omega)$ is

0021-9991/79/120397-08$02.00/0

calculated on this mesh. Finally, the contours for which $\mathrm{Re}(g) = 0$ and for which $\mathrm{Im}(g) = 0$ are plotted on a single plot. In the absence of singularities, the intersections of the two contours correspond to the desired roots.

When isolated singularities or branch cuts are present, additional intersections may appear on the plot. For example, a branch cut will appear as a zero contour of $\mathrm{Re}(g)$ if the values of $\mathrm{Re}(g)$ are of opposite sign on either side of the branch cut. To distinguish between those intersections that are roots and those that are singularities, the local variation of g must be examined.

3. Examples

Two closely related examples from plasma physics [2] are given here. Both concern finding the complex frequencies characteristic of collisionless drift modes in a hydrogen plasma. A slab model is assumed with a density gradient and magnetic shear but no temperature gradients. The drift modes are then described as solutions to an ordinary differential equation (with appropriate boundary conditions), in which the characteristic frequencies appear as generalized eigenvalues. In the first example the eigenvalues are found as roots of an analytic dispersion relation, which results from an approximate solution to the differential equation. In the second example the differential equation is solved directly to obtain the eigenvalues.

These examples illustrate several points. First, they demonstrate the effectiveness of the graphical method for finding roots in the presence of considerable structure. Second, the versatility of the method is displayed; it can be used not only to find roots of nonlinear equations but also to obtain generalized eigenvalues of differential equations. Finally, since one example is an approximation to the other, the validity of the approximation can be assessed.

3.1. *Roots of Algebraic Equations*

By using the method of matched asymptotic expansions [3] and by considering only even modes, the complex eigenvalues, ω, are found to satisfy the following dispersion relation:

$$1 - \frac{\sigma_0}{2\pi(i\mu)^{1/2}}\,\Gamma\left(\frac{1}{4} - \frac{i\Lambda}{4\mu}\right)\Gamma\left(\frac{1}{4} + \frac{i\Lambda}{4\mu}\right)\sin\left[\frac{\pi}{4}\left(1 + \frac{i\Lambda}{\mu}\right)\right]\ln(x_e\mu^{1/2}) = 0. \quad (1)$$

This is just Eq. (2) of Ref. [2] with spurious factors of 4 and $2^{1/2}$ removed (consistent with the derivation in Ref. [3]). Branch cuts for the square root and logarithm functions are taken to lie along the negative real axis, i.e., the principal branches are chosen.

All quantities appearing above (except for S) are as defined in Ref. [2]:

$$\Lambda \equiv \tilde{\rho}_i^{-2} D^{-1}\{\omega[1 + \tau(1 - \Gamma_0)] - \omega_* \Gamma_0\}, \quad (2)$$

$$\mu \equiv \tilde{\rho}_i^{-2} S^{1/2} \frac{L_n}{L_s} \frac{\omega_*}{\omega\tau}, \tag{3}$$

$$\sigma_0 \equiv i\pi^{1/2} x_e \tilde{\rho}_i^{-2} D^{-1}(\omega - \omega_*), \tag{4}$$

$$x_e \equiv \frac{\tau^{1/2}\tilde{\rho}_i}{(2M/m)^{1/2}(L_n/L_s)} \frac{\omega}{\omega_*}, \tag{5}$$

$$D \equiv (\omega\tau + \omega_*)(\Gamma_0 - \Gamma_1), \tag{6}$$

$$S \equiv D^{-1}\omega(1 + \tau). \tag{7}$$

The expression for S has been revised here to apply for arbitrary values of ω_*[4]. The Γ appearing in Eq. (1) is the complex gamma function, while Γ_j is defined as

$$\Gamma_j \equiv e^{-b} I_j(b), \tag{8}$$

where I_j is the modified Bessel function. The remaining quantities above are treated as parameters: M/m, τ, L_n/L_s, and b are specified; $\tilde{\rho}_i$ cancels out; and ω_* can be used to normalize ω. Here the normalizing frequency will be taken to be

$$\omega_s \equiv (\tau b)^{1/2}\omega_* . \tag{9}$$

By making use of the identities,

$$\Gamma(z + 1) = z\Gamma(z) \tag{10}$$

and

$$\Gamma(z)\,\Gamma(1 - z) = \frac{\pi}{\sin \pi z}, \tag{11}$$

and upon multiplying by $\tilde{\rho}_i^2 D(\Lambda + i\mu)$, the dispersion relation becomes

$$g(\omega) \equiv \tilde{\rho}_i^2 D \left\{\Lambda + i\mu - 2G\sigma_0 \left(\frac{i\mu}{\pi}\right)^{1/2} \ln(x_e \mu^{1/2})\right\} = 0, \tag{12}$$

where

$$G \equiv \pi^{1/2}\Gamma\left(\frac{5}{4} - \frac{i\Lambda}{4\mu}\right) \Big/ \Gamma\left(\frac{3}{4} - \frac{i\Lambda}{4\mu}\right). \tag{13}$$

Equation (12) is the nonlinear equation that is solved here. It differs from the perturbation theory result (Eq. (3) of Ref. [2]) only through the factor G.

With the following choice of parameters—$M/m = 1836$, $\tau = 1$, $L_n/L_s = 0.05$, and $b = 0.5$—the plot of the zero contours of Re(g) (solid) and Im(g) (dotted) is as shown in Fig. 1. Numerous intersections are apparent. Those marked with o's are roots, while those marked with $*$'s are isolated singularities lying on a branch cut.

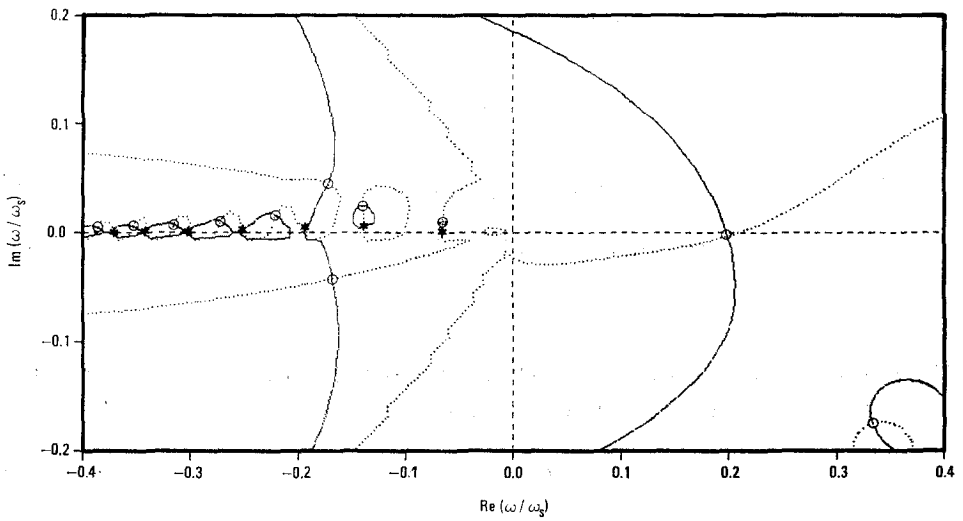

FIG. 1. Zero contours of Re(g) and Im(g) for first example.

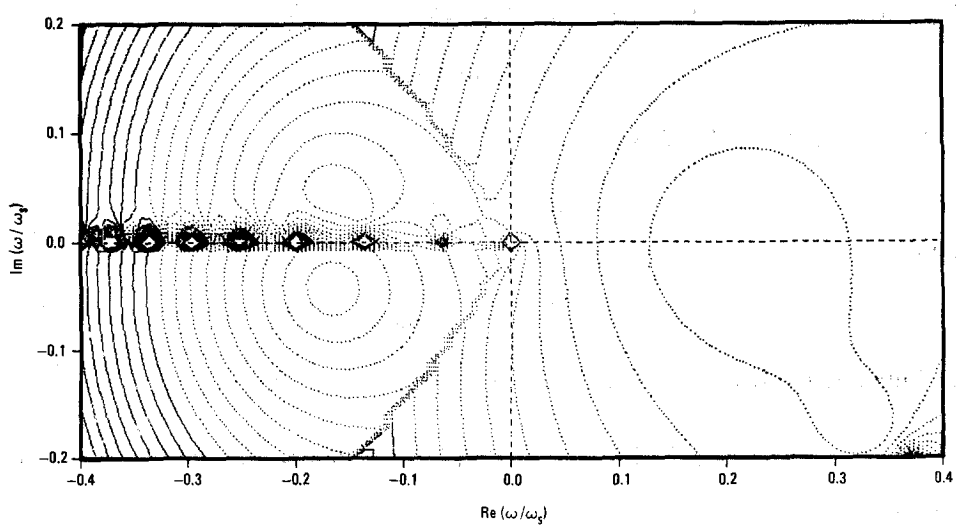

FIG. 2. Contours of $|g| - 1$ for first example.

This identification is facilitated by examining a contour plot of $|g| - 1$, which is shown in Fig. 2. Negative contours are dotted, while zero or positive contours are solid. Hence, roots appear as dotted bull's-eyes; isolated singularities appear as solid bull's-eyes; and branch cuts appear as linear features.

Figures 1 and 2 were generated by calculating the g values on a 101 × 51 mesh in the ω-plane. On a CDC 7600 computer, the g calculation required 4 sec of CPU time, while the contour plotting took another 2 sec.

3.2. *Eigenvalues of Differential Equation*

The differential equation for collisionless drift modes in a plasma slab without temperature gradients is (Eq. (4) in Ref. [2])

$$\tilde{\rho}_i^2(\Gamma_0 - \Gamma_1)\frac{x_i}{x}Z\left(\frac{x_i}{x}\right)\frac{\partial^2\phi}{\partial x^2} + \left\{\frac{\omega - \omega_*}{\tau\omega + \omega_*}\left[1 + \frac{x_e}{x}Z\left(\frac{x_e}{x}\right)\right] + 1 + \frac{x_i}{x}Z\left(\frac{x_i}{x}\right)\Gamma_0\right\}\phi = 0, \tag{14}$$

and the boundary conditions for even modes are

$$\phi'(o, \omega) = 0, \tag{15}$$

$$\phi(\infty, \omega) = 0. \tag{16}$$

The dependent variable, ϕ, is the perturbed electrostatic potential, which is complex, while the independent variable, x, is the coordinate in the direction of the density gradient. The remaining quantities in Eq. (14) have been defined previously except for

$$x_i \equiv (M/m)^{1/2}\tau^{1/2}x_e \tag{17}$$

and Z, which is the plasma dispersion function [5].

The standard method for solving Eq. (14) is as follows [6]. A value for ω is assumed, and a relatively large distance, x_b, is chosen for which the WKB approximation gives an accurate solution, $\phi(x_b, \omega)$, consistent with the second boundary condition [Eq. (16)]. Applying the Numerov difference scheme to Eq. (14), one "shoots" from x_b to 0. The value of ω is then adjusted by Newton's method, and the shooting procedure is repeated until the first boundary condition [Eq. (15)] is satisfied.

To apply the graphical method, one defines

$$g(\omega) \equiv \phi'(0, \omega) \tag{18}$$

and carries out the above procedure except for the Newton's method iteration. For the same parameter values as in the first example, the plot of the zero contours of Re(g) and Im(g) is as shown in Fig. 3. By examining Fig. 4, the intersections can be categorized as roots (o's), isolated singularities ($\times$'s), or branch cuts ($+$'s). The latter distinction is significant, since the isolated singularities correspond to the odd-mode solutions of Eq. (14). The complete spectrum of even and odd modes is thus obtained using the graphical method.

The cost of calculating the g values for this example is understandably greater than for the first example, since meshes in x as well as in ω are required. An x-mesh characterized by 501 points and a shooting distance of $x_b = 10\,\tau^{1/2}\tilde{\rho}_i$ was found to be adequate, while a 41 $\times$ 21 mesh was used in the ω-plane. The resulting CPU time on a CDC 7600 computer was 70 sec.

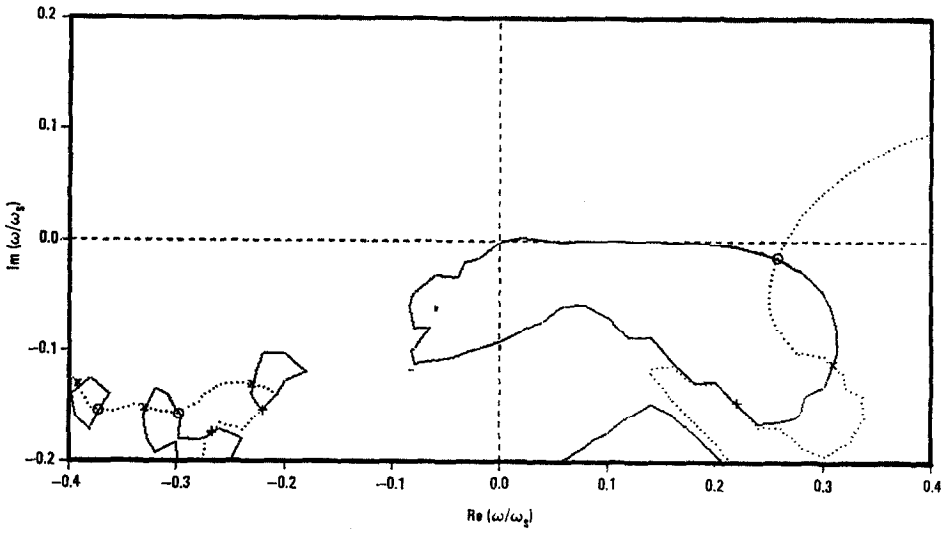

FIG. 3. Zero contours of Re(g) and Im(g) for second example.

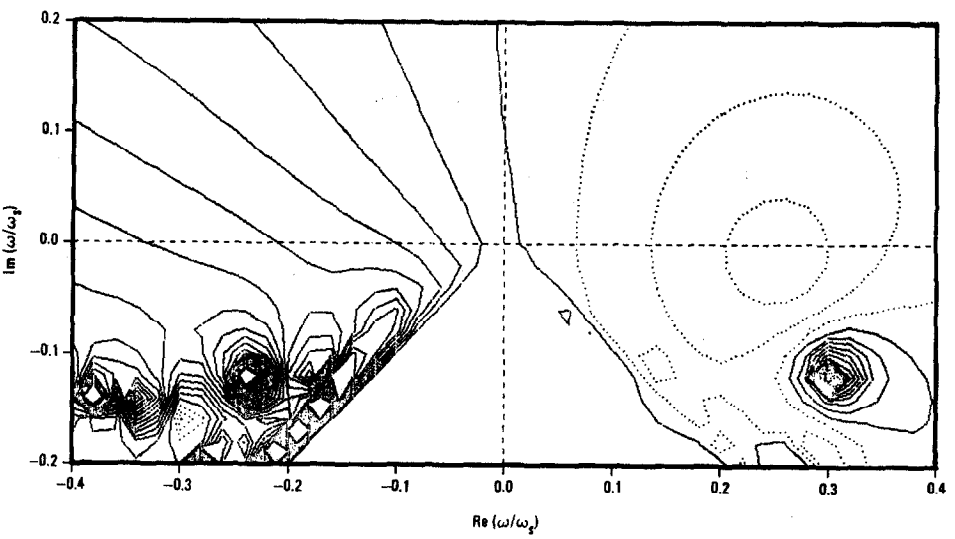

FIG. 4. Contours of $|g| - 1$ for second example.

Since the two examples are closely related, it is instructive to compare the numerical values obtained for the roots. These are given in Tables I and II and were confirmed by iterating with Newton's method. Depending upon whether Re(ω) is positive or negative, the roots correspond to either electron or ion drift modes. Evidently the only root for which the tabulated values are in even rough agreement is that for the electron drift mode that is most unstable, i.e., that has the largest value for Im(ω).

TABLE I

Roots for first example.

$\mathrm{Re}(\omega/\omega_s)$	$\mathrm{Im}(\omega/\omega_s)$
0.20	0.004
0.33	−0.17
−0.07	0.011
−0.14	0.025
−0.17	0.044
−0.17	−0.043
−0.22	0.016
−0.27	0.010
−0.32	0.007
−0.35	0.005
−0.39	0.004

Note: All roots above correspond to even modes.

TABLE II

Roots for second example

$\mathrm{Re}(\omega/\omega_s)$	$\mathrm{Im}(\omega/\omega_s)$	Parity
0.26	−0.016	Even
0.30	−0.12	Odd
−0.23	−0.13	Odd
−0.30	−0.16	Even
−0.33	−0.15	Odd
−0.37	−0.15	Even
−0.38	−0.14	Odd

This root is the one that the approximate solution is intended to predict. With the choice of parameters made here, the approximation is apparently not valid for the ion drift modes.

ACKNOWLEDGMENTS

I am grateful to R. E. Waltz for suggesting the examples and to R. H. Davidson for assistance in generating the contour plots. This work was supported by Department of Energy Contract No. EY-76-C-03-0167, Project Agreement No. 38.

REFERENCES

1. P. HENRICI, "Elements of Numerical Analysis," Wiley, New York, 1964.
2. K. T. TSANG, P. J. CATTO, J. C. WHITSON, AND J. SMITH, *Phys. Rev. Lett.* **40** (1978), 327.
3. P. J. CATTO AND K. T. TSANG, Oak Ridge National Laboratory Report, ORNL/TM-6045, 1977.
4. R. DOMINGUEZ, personal communication.
5. B. D. FRIED AND S. D. CONTE, "The Plasma Dispersion Function," Academic Press, New York, 1961.
6. N. T. GLADD AND W. HORTON, JR., *Phys. Fluids* **16** (1973), 879.

RECEIVED: October 9, 1978; REVISED: February 1, 1979

WAYNE PFEIFFER

General Atomic Company
San Diego, California 92138